JOURNAL OF VIROLOGY, Mar. 1989, p. 1326–1337
0022-538X/89/031326-12$02.00/0

Vol. 63, No. 3

Mutagenesis of the In-Frame Opal Termination Codon Preceding nsP4 of Sindbis Virus: Studies of Translational Readthrough and Its Effect on Virus Replication

GUANGPU LI AND CHARLES M. RICE*

Department of Microbiology and Immunology, Washington University School of Medicine, Box 8093, 660 South Euclid Avenue, St. Louis, Missouri 63110-1093

Received 13 October 1988/Accepted 28 November 1988

Sindbis virus (SIN) contains an in-frame opal termination codon in the nonstructural protein-coding region separating nsP3 and nsP4 and provides a useful tool to study the readthrough phenomenon of the termination codon in host cells and its role in viral replication. We have changed the opal codon by site-directed mutagenesis of a full-length SIN cDNA clone to either sense amino acids (serine, tryptophan, or arginine) or the other two translation termination codons (amber or ochre). Transcripts from all of the mutant cDNA clones were infectious when used to transfect chicken embryo fibroblasts. The resulting progeny virus stocks were then used to study the effects of these mutations on viral protein and RNA synthesis, growth properties, host range, and fitness compared with the parental strain. None of the mutants showed temperature sensitivity in plaquing efficiency or plaque morphology on chicken embryo fibroblast monolayers. Relative to the wild-type parent, the mutants containing sense replacements overproduced nsP34 but not nsP4 and made slightly decreased levels of nsP3, with a delay in its appearance. This indicates that the cleavage separating nsP3 and nsP4 occurs in these mutants and also that the level of nsP4 is not regulated solely by readthrough of the opal codon. The amber and ochre mutants produced decreased levels of nsP34, and the ochre mutant grew significantly more slowly than the other mutants or wild-type virus. For all five mutants, RNA synthesis early in infection was inhibited compared with that of the parental virus. This effect was apparent at multiplicities of infection of 20 PFU per cell but not at 100 PFU per cell. Using in situ hybridization to distinguish between mutant and wild-type plaques, we have studied the behavior of the serine mutant in a high-multiplicity growth competition experiment with wild-type virus. The wild-type virus eventually outcompeted the mutant after several passages, and these results indicate that this mutation has resulted in effects that are at least partially *cis* acting. Furthermore, by studying the growth, plaque formation, and protein synthesis of the mutants in various cell types, we have observed host range effects of the mutations, especially in mosquito and human cells. In addition, we have demonstrated, at least indirectly, that opal, amber, and ochre termination codons in the SIN nucleotide context can be suppressed in cultured cells of chicken, human, hamster, and mosquito origin.

Readthrough of termination codons is employed by many RNA viruses, including Qβ bacteriophage (UGA), alphaviruses (UGA), retroviruses (UAG), and some plant viruses (UAG), to regulate the synthesis of some essential viral proteins (14, 34, 35, 40, 42, 44, 50, 53, 54). In most of these viruses except Qβ phage, the in-frame termination codons are located upstream of the putative viral RNA replicases or reverse transcriptases. Therefore, readthrough plays an important role in allowing virus replication to occur. In this report, we have used Sindbis virus (SIN) as a model system to examine the readthrough of termination codons in animal cells. We have also studied the regulatory function of the SIN in-frame opal termination codon in terms of production of viral nonstructural protein readthrough products and their effects on subsequent RNA amplification.

SIN is an enveloped positive-strand RNA virus (for a recent review, see reference 45) that infects a variety of vertebrate and invertebrate hosts (4, 8, 28, 47). It is the type virus of the *Alphavirus* genus which belongs to the family *Togaviridae*. The SIN genomic 49S RNA serves as an mRNA for production of four nonstructural proteins (called nsP1 to -4) numbered in order of their location in the genome (44). Although their roles in RNA replication have not been firmly established, the nonstructural proteins are believed to be components of the RNA replicase-transcriptase machinery that initiates viral RNA replication by the synthesis of a minus-strand 49S RNA complementary to the incoming genomic plus-strand 49S RNA. This minus-strand in turn serves as the template for the synthesis of additional plus-strand genomic 49S RNA and a 3′ coterminal subgenomic 26S RNA that acts as the mRNA for the production of the SIN structural proteins.

The translation of SIN nonstructural proteins starts from a single AUG codon at the beginning of nsP1, and the four nonstructural proteins are produced by cotranslational and posttranslational proteolytic cleavages (16). The last nonstructural protein, nsP4, is highly conserved among alphaviruses and shares homologous amino acid sequences with the RNA-dependent RNA replicase of poliovirus and nonstructural proteins of other positive-strand plant and animal RNA viruses (17, 22, 37). Therefore, it has been postulated that nsP4 is the replicase subunit containing the elongating activity for the SIN RNA-dependent RNA polymerase (22). This contention is supported by the existence of an SIN RNA-negative temperature-sensitive (*ts*) mutant, *ts*6 (5), which grows well at 30°C but upon shift to 40°C shuts off all

* Corresponding author.

RNA synthesis (2, 23, 39). This lesion has been mapped to the nsP4-coding region (15). In the SIN genome, however, there is an in-frame opal termination codon separating nsP3 and nsP4 (43, 44). Therefore, the nsP4-coding region can be translated only by a readthrough mechanism to produce nsP4 and nsP34 (16, 45). Among alphaviruses, Middelburg virus (43) and Ross River virus also contain in-frame opal termination codons in positions analogous to that of SIN (42). In contrast, Semliki Forest virus (SFV) (46) and O'-Nyong-nyong virus (42) do not contain the opal codon and instead have an arginine codon at that position.

The in vitro transcripts from some full-length cDNA clones of SIN are able to initiate a complete infectious cycle upon transfection into appropriate host cells (36). By directed mutagenesis of such cDNA clones, we have begun a study of the structure-function relationships of SIN nonstructural proteins and RNA sequences. To investigate the regulatory function of the opal codon and the effect of altered levels of nsP3, nsP4, and nsP34 on viral RNA replication, we have constructed a series of mutations of the opal codon preceding nsP4. In this paper, we report the characterization of these mutants.

MATERIALS AND METHODS

Enzymes and plasmids. All restriction enzymes, T4 DNA ligase, *Escherichia coli* exonuclease III, and *E. coli* DNA polymerase I and its large fragment (Klenow) were obtained from New England BioLabs, Inc., Bethesda Research Laboratories, Inc., Boehringer Mannheim Biochemicals, or Promega Biotec. Avian myeloblastosis virus reverse transcriptase was from Life Sciences, Inc., and dCTPαS was from New England Nuclear (Dupont). All radioactive materials were purchased from either Amersham Corp. or ICN Pharmaceuticals Inc. Plasmid pGC2 (32) and phage M13k07 (48) were generous gifts from Douglas Berg (Department of Microbiology and Immunology, Washington University School of Medicine). The monospecific antisera against nsP1 to -4 of SIN (16) were kindly provided by W. Reef Hardy and James H. Strauss (Biology Division, California Institute of Technology).

Cell cultures and viruses. Chicken embryo fibroblasts (CEF), BHK-21 cells (from ATCC via Robert E. Johnston, North Carolina State University), SW-13 cells (human adenocarcinoma cells from ATCC), and C7-10 cells (*Aedes albopictus* cell line, from Victor Stollar, University of Medicine and Dentistry of New Jersey) were propagated as previously described (10, 21, 41; T. J. Chambers, D. W. McCourt, and C. M. Rice, Virology, in press). All virus stocks were derived from either the full-length SIN cDNA clone Toto1000 or its mutagenized derivatives by in vitro transcription of plasmid DNA with SP6 polymerase followed by RNA-mediated transfection of CEF cells (36). In this paper, wild-type or parental virus refers to the virus stock derived from SIN cDNA clone Toto1000, while serine, tryptophan, arginine, amber, and ochre mutants refer to the virus stocks derived from mutagenized Toto cDNA clones Toto1000.S, Toto1000.W, Toto1000.R, Toto1000.Am, and Toto1000.Oc, respectively (see below for plasmid construction details).

Plaque assays. Virus stocks were grown and the titers were determined on CEF monolayers as described previously (41). Plaque assays with CEF, BHK-21, and SW-13 cells were conducted under the same conditions (41), while plaque formation on C7-10 cells at 34.5°C was assayed by a method described by Durbin and Stollar (10).

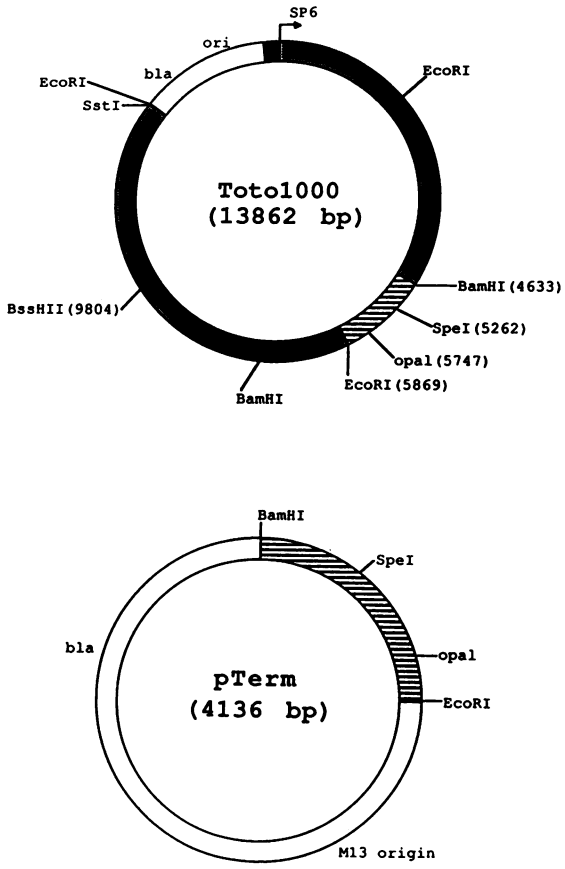

FIG. 1. Plasmid constructions. Shown are plasmids used for the production of infectious RNA transcripts (Toto1000) and in vitro mutagenesis (pTerm). Details of the construction of the Toto1000 opal substitution mutants are described in Materials and Methods. The *Bam*HI-*Eco*RI restriction fragment containing the opal termination codon between nsP3 and nsP4 (▨) was subcloned from Toto1000 to the polylinker region of pGC2 (32) to produce pTerm. After mutagenesis, the *Spe*I-*Eco*RI restriction fragment from each of the mutagenized pTerm constructs was recloned back into Toto1000 in a three-fragment ligation reaction, using the *Eco*RI-*Bss*HII and *Bss*HII-*Spe*I fragments of Toto1000. The positions of the restriction sites in the SIN genome (44) used for these constructions are indicated. In Toto1000, the SIN cDNA sequence (▭) and the SP6 polymerase promoter sequence used for production in vitro of RNA transcripts (▬) are shown.

Plasmid constructions and site-directed mutagenesis. A schematic of Toto1000 showing the restriction sites used for mutagenesis and subcloning is shown in Fig. 1. Briefly, the *Bam*HI-*Eco*RI fragment from Toto1000, which contains the in-frame opal termination codon, was subcloned into pGC2 (32), resulting in the plasmid called pTerm (Fig. 1). pTerm contains the M13 replication origin, and with the helper phage M13k07, single-stranded pTerm DNA was packaged and isolated as previously described (48). Five mutagenic oligonucleotides (Fig. 2) were chemically synthesized and used to change the opal codon to a serine, tryptophan, arginine, amber, or ochre codon.

Serine and tryptophan mutations were generated by using a standard in vitro site-directed mutagenesis procedure as described previously (58), while arginine, amber, and ochre mutations were produced by a modified method developed by Nakamaye and Eckstein (33). Clones containing the

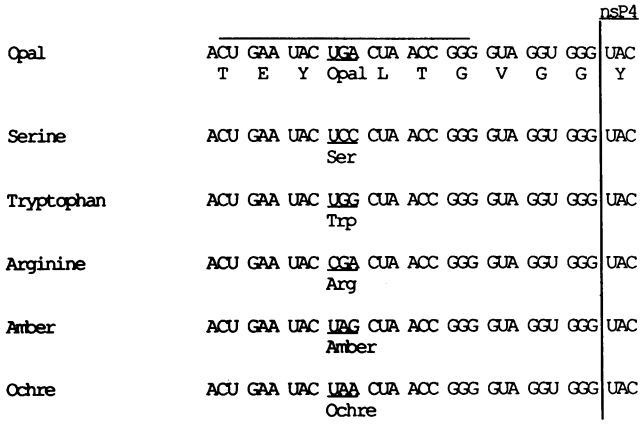

FIG. 2. Nucleotide and amino acid sequences in the mutagenized region. The nucleotide sequence (from nt 5739 to 5771 in SIN genome) and the deduced amino acid sequence for the wild-type virus and the five opal substitution mutants are shown. Opal, Wild-type virus derived from SIN cDNA clone Toto1000; serine, tryptophan, arginine, amber, and ochre mutants derived from corresponding mutagenized Toto clones. The viral RNA sequences were determined by a modified dideoxy-chain termination method (55). The line above the nucleotide sequence of opal denotes the location of the five oligonucleotides (20-mer) used for mutagenesis which are complementary to each mutant sequence shown. The mutant codons are underlined. The start of SIN nsP4 is assigned tentatively by homology with SFV nsP4 (46).

desired mutations were identified by colony hybridization (29) and DNA sequencing (38).

The *Spe*I-*Eco*RI restriction fragments containing the mutagenized region were isolated and purified on low-melting-temperature agarose gels (51) and were recloned back to Toto1000 in a three-fragment ligation reaction. The *Eco*RI, *Bss*HII, and *Spe*I restriction sites of Toto1000 were used to generate the other two fragments (*Eco*RI-*Bss*HII and *Bss*HII-*Spe*I) for this construction as shown in Fig. 1. The five mutagenized Toto1000 derivatives were named Toto1000.S, Toto1000.W, Toto1000.R, Toto1000.Am, and Toto1000.Oc with respect to the substitutions of the opal codon by serine, tryptophan, arginine, amber, and ochre codons, respectively.

Nucleotide sequence analysis. Prior to in vitro transcription, the sequence of the entire region between the *Spe*I-*Eco*RI DNA sites of plasmids Toto1000.S, Toto1000.W, Toto1000.R, Toto1000.Am, and Toto1000.Oc was verified by either the chemical sequencing method (30) or the chain termination method (38). The existence of the original mutations in in vivo-replicated RNAs was confirmed by direct sequencing of virus-specific RNAs (55) that were isolated from virus-infected CEF cells (52) and purified by oligo(dT) cellulose chromatography.

Growth rates in CEF cells. The secondary CEF monolayers in 35-mm dishes were infected with the virus stocks at a multiplicity of infection (MOI) of either 20 or 100 PFU per cell in 200 μl of phosphate-buffered saline containing 1% fetal calf serum (FCS). The plates were incubated at 37°C, and virus samples were collected at 3, 6, 9, and 12 h postinfection, and the titers were then determined on secondary CEF monolayers.

In vivo protein analysis, immunoprecipitation, and sodium dodecyl sulfate-polyacrylamide gel electrophoresis (SDS-PAGE). All incubations were done at 37°C except where otherwise indicated. Secondary CEF monolayers in 35-mm dishes were infected with wild-type virus or mutants in 200 μl of phosphate-buffered saline containing 1% FCS at an MOI as indicated. The plates were incubated at 4°C for 1 h with occasional rocking. The infection mixture was then removed, and 2 ml of Eagle minimal essential medium–Earle salts containing 3% FCS was added and incubated for the indicated periods. The medium was then replaced with 2 ml of Eagle minimal essential medium–Earle salt (3% FCS) lacking methionine. After incubation for 30 min, the medium was removed and 0.5 ml of Eagle minimal essential medium (3% FCS)–Earle salts lacking methionine but containing [^{35}S]methionine at a final concentration of 40 μCi/ml was added. The plates were then labeled and chased at 37°C for the indicated periods. After being washed with ice-cold phosphate-buffered saline twice, the cell monolayers were lysed with 200 μl of 1% SDS containing 40 μg of phenylmethylsulfonyl fluoride per ml, heated to 90°C for 5 min, and stored at −70°C. The lysates were either directly analyzed by 10% SDS-PAGE (26) or were used for an immunoprecipitation assay (1, 16). Immunoprecipitates were denatured by being heated at 95°C for 3 min and were then separated by 6% SDS-PAGE. Gels were treated for fluorography (27), dried, and exposed to X-ray film.

RNA analysis by RNase protection. Secondary CEF cells in 60-mm dishes were infected as described above with wild-type virus or mutants at 20 or 100 PFU per cell in 400 μl of phosphate-buffered saline containing 1% FCS. At different times postinfection, the cytoplasmic RNAs were isolated (52) and analyzed in an RNase protection assay with a virus-specific RNA probe (56). An RNA probe 243 nucleotides (nt) in length, including a 215-base sequence complementary to the junction region of SIN 49S genomic RNA (nt 7501 to 7716) (see Fig. 6C), was made by in vitro transcription of a *Ssp*I-linearized plasmid called pGem-J1 (M. Jones, unpublished data), using SP6 polymerase and [α-^{32}P]CTP as a label (31).

The assay was conducted as follows. A 100-ng sample of isolated cytoplasmic RNAs was hybridized with >20-fold excess RNA probe (5×10^5 cpm) by being heated at 90°C for 10 min and then incubated at 55°C for 18 h in 20 μl of annealing buffer containing 40 mM PIPES [piperazine-*N*,*N*′-bis(2-ethanesulfonic acid), pH 6.4]–400 mM NaCl–1 mM EDTA–80% deionized formamide. Upon completion, the annealing reaction was quickly diluted into 200 μl of RNase solution (10 mM Tris [pH 7.5]–5 mM EDTA–300 mM NaCl–40 μg of boiled RNase A per ml) and was incubated at 37°C for 20 min. SDS and proteinase K were then added to final concentrations of 0.1% and 150 μg/ml, respectively, and incubation was continued at 37°C for 15 min. After phenol-chloroform extractions and ethanol precipitation, the pellet was suspended in 20 μl of sample buffer (80% deionized formamide–50 mM Tris borate–1 mM EDTA [pH 8.3]–0.1% xylene cyanol–0.1% bromophenol blue), was heated to 95°C for 2 min, and was run on 5% polyacrylamide-urea sequencing gels (30). After electrophoresis, gels were fixed in 10% acetic acid–12% methanol for 10 min and were dried. Virus-specific protected RNA bands were localized by autoradiography, cut out from the gel, and quantitated by liquid scintillation counting.

Competition assay and in situ hybridization to SIN plaques. Wild-type virus and the serine mutant were mixed at an equal MOI, and the virus mixture was passaged on secondary CEF monolayers (37°C) in 35-mm dishes at either a high MOI (100 PFU per cell) or a low MOI (0.01 PFU per cell) for six serial passages. Wild-type virus and the serine mutant alone were passaged in parallel as negative and positive

controls, respectively. At each passage, the culture supernatant was harvested at 12 h postinfection and used for the in situ hybridization assay.

The hybridization of SIN plaques described below is adapted from a method of Villarreal and Berg (49) for hybridization to plaques formed by a DNA virus (simian virus 40). Secondary CEF monolayers in 100-mm dishes were infected by the virus mixtures obtained from each passage at dilutions sufficient to produce about 400 to 500 plaques per plate. The agarose overlay was removed carefully, and a dry nitrocellulose filter was laid on top of the cell monolayer. The filter was moistened by blotting with a paper towel wetted with 50 mM Tris hydrochloride (pH 7.5)–0.15 M NaCl. The filter, with adherent cells, was then peeled off the plate with forceps. Lysis of the cell monolayer and released virus and immobilization of the RNA on the filter were accomplished by placing the nitrocellulose filter in a puddle (0.8 ml) of 0.5% Brij 35–0.5% deoxycholate (3) on plastic wrap for 1 min (cell side up) and blotting the filter briefly on a paper towel. After this step was repeated, the filter was then placed onto the same volume of 1.5 M NaCl–0.5M Tris hydrochloride (pH 7.5) for 5 min and finally was equilibrated twice with 20× SSC (1× SSC is 0.15 M NaCl plus 0.015 M sodium citrate) (for 5 min) by the same procedure. The filter was then air dried for 30 min at room temperature and then baked at 80°C for 2 h in a vacuum oven. The membrane was prehybridized in 6 ml of 10× Denhardt solution–6× SSC–0.2% SDS–100 μg of salmon sperm DNA per ml at 42°C for at least 6 h in a sealed polypropylene bag. The 5′-^{32}P-labeled mutagenic oligonucleotide (opal-serine) probe (5×10^6 cpm/ml) was added. The bag was resealed and incubated at 42°C for another 12 to 18 h. After hybridization, the filter was first washed at low stringency (2× SSC, room temperature) for 30 min followed by autoradiography of the moist filter; all plaques gave a positive signal under these washing conditions. The same filter was then washed twice at higher stringency (1× SSC at 42°C; 15 min per wash) and was reexposed. Under these conditions, only serine mutant plaques (homologous hybridization) were positive.

RESULTS

Infectivities and growth rates of the mutants compared with those of the parental virus. Toto1000 derivatives containing mutations changing the opal codon preceding nsP4 to serine, tryptophan, arginine, amber, or ochre were constructed and checked by sequence analysis as described in Materials and Methods. After restriction digestion of the plasmid DNAs with *Sst*I to produce runoff transcripts, SP6 polymerase was used to produce 5′-capped in vitro transcripts. RNA transcripts from all five mutagenized Toto cDNA clones were infectious upon diethylaminoethyl-dextran-mediated transfection of secondary CEF monolayers, as determined by cytopathic effects and plaque assays. The specific transfectivities of the transcripts from Toto1000 and its mutagenized derivatives were not significantly different (about 10 to 20 PFU/ng). The wild-type virus and the mutants also had similar plaque morphologies on CEF monolayers (data not shown).

For the growth rate assays, secondary CEF monolayers were infected with wild-type virus or the mutants at either 20 or 100 PFU per cell. Samples of the culture medium were harvested at the indicated times, and titers were determined by plaque assay. All mutants grew to titers of $>10^9$ PFU/ml

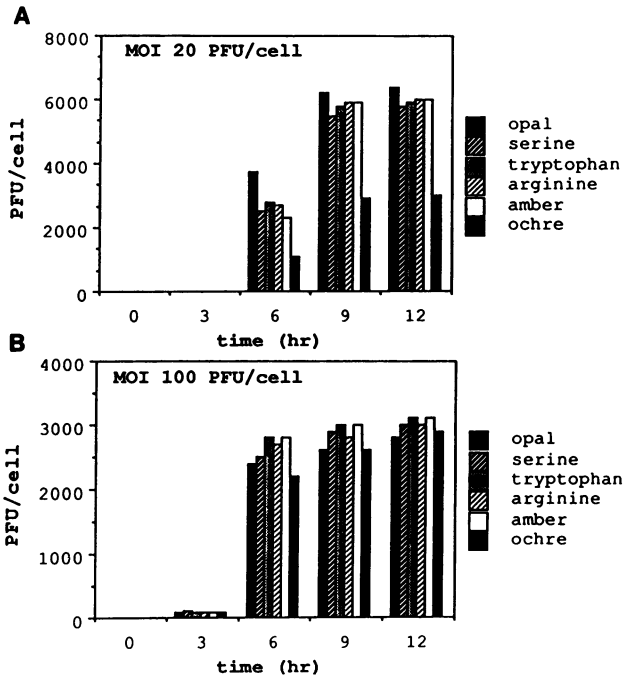

FIG. 3. Viral growth rate in CEF. CEF monolayers were infected with wild-type virus (opal) and the five mutants at either 20 (A) or 100 (B) PFU per cell. Virus samples were collected at the indicated times, and titers were determined by plaque assay on CEF monolayers. The data shown are average numbers from two independent experiments.

(~1,000 PFU per cell), and the mutations appeared to be stable as confirmed by sequencing virus-specific RNAs isolated from virus-infected cells after three serial passages (data not shown). The formal possibility of second-site reversion(s) or low levels of same-site reversion (<10 to 20%) could not be ruled out by these analyses. At 20 PFU per cell, the mutants, especially the ochre mutant, grew more slowly than the wild-type virus at early times after viral infection (Fig. 3A), suggesting that the mutations have negative effects on virus replication. In contrast (Fig. 3B), there was no significant difference between the wild-type and mutant growth rates at 100 PFU per cell.

Since the opal codon was replaced by either sense or other termination codons, we expected that the sense mutants might overproduce the readthrough product nsP4 (as well as nsP34) and decrease the amount of nsP3 to some extent, depending on the cleavage efficiency between nsP3 and nsP4. The amber and ochre mutants might also change the level of nsP4, depending on their readthrough efficiencies. These altered levels of the nonstructural proteins or changes in their activity due to amino acid replacements at the opal codon could then lead to changes in the efficiency of RNA replication.

Immunoprecipitation assays of viral nonstructural proteins. We examined differences in nonstructural protein patterns between the wild-type and the mutant viruses (Fig. 4 and 5). These experiments were conducted at a high MOI (100 PFU per cell) to avoid the differences in the rate of wild-type virus versus mutant replication which were apparent at lower MOIs. After infection of secondary CEF monolayers with either the wild-type virus or the mutants, the accumulation of viral proteins was examined in a long labeling period (Fig. 4), and the production and stability of the nonstructural

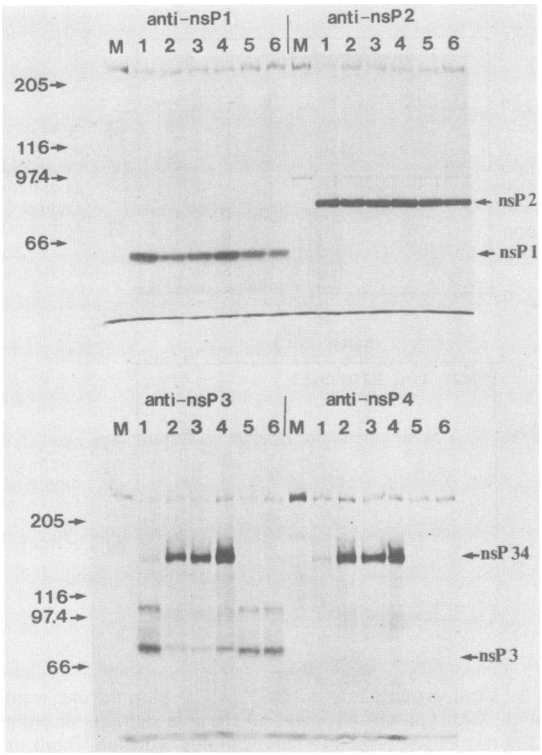

FIG. 4. Immunoprecipitation of viral nonstructural proteins in a steady-state labeling experiment. CEF monolayers were infected with the wild-type virus and the five mutants at 100 PFU per cell. At 2 h postinfection, the cells were labeled with [^{35}S]methionine for 3 h and were then lysed with 1% SDS. The lysates were immunoprecipitated with SIN polyclonal antibodies monospecific for nsP1, nsP2, nsP3, and nsP4 and were analyzed by 6% SDS-PAGE. nsP4 was not detected because of the low levels found in SIN-infected cells (16). The reactivity of the nsP4 antisera with the nsP4 domain in these experiments can be seen by the efficient precipitation of nsP34 (see also the discussion in the text). The protein samples in lanes M, 1, 2, 3, 4, 5, and 6 were isolated from cells which were mock infected or infected with wild-type, serine mutant, tryptophan mutant, arginine mutant, ochre mutant, or amber mutant virus, respectively. Molecular mass standards (in kilodaltons) are indicated on the left, and the positions of the SIN nonstructural proteins are indicated on the right.

proteins were examined in a pulse-chase experiment (Fig. 5). Nonstructural proteins were identified by immunoprecipitation with region-specific antisera for each nonstructural protein (16). After 3 h of continuous labeling from 2 to 5 h postinfection, the levels of nsP34 produced by the serine, tryptophan, and arginine mutants were about five- to eightfold higher than that of the wild-type virus, while the levels of nsP3 of these three mutants were two- to threefold lower. The amber and ochre mutants, on the other hand, underproduced nsP34 but not nsP3 (Fig. 4). The levels of nsP1 and nsP2 were similar for the wild-type virus and all the mutants and therefore served as internal controls for comparing the levels of nsP3 and nsP34 (Fig. 4). In a pulse-chase experiment (Fig. 5), the serine mutant again showed the overproduction of nsP34 and a delay in the appearance of nsP3 by more than 15 min. The amber and ochre mutants showed reduced levels of nsP34 compared with the wild-type virus. The tryptophan mutant (and presumably the arginine mutant also, although this was not tested) had the same pulse-chase pattern as the serine mutant (data not shown). Although the serine, tryptophan, and arginine mutants overproduced the readthrough product nsP34, we were not able to detect a significant increase in the amount of nsP4. We do not believe that this result was due to the inability of the nsP4 antisera to recognize the cleaved nsP4 product, for several reasons. First, low levels of nsP4 have been detected in SIN-infected cells with this antisera when larger fractions of the lysate were immunoprecipitated (16). Second, the nsP4 antisera reacted efficiently with nsP34. Finally, we have shown that this antisera readily immunoprecipitated nsP4 from SFV-infected lysates (results not shown; similar concentrations of the antisera were used for both experiments).

In the pulse-chase experiment, multiple forms of SIN nsP3 were observed (see also reference 16). During a 10-min pulse, the nsP3 appeared as a single labeled band on 6% SDS-PAGE. The amount of this species decreased with time and was gradually chased into two larger forms (by approximately 2 and 30 kilodaltons) within 2 h (Fig. 5). These larger forms of nsP3 have been shown to be due to posttranslational phosphorylation (G. Li et al., manuscript in preparation).

Analysis of RNA and protein synthesis early in infection. To study whether the imbalanced production of nsP3 and nsP34 by the mutants had detectable effects on viral RNA and protein synthesis early in the infectious cycle, we isolated virus-specific intracellular RNAs and proteins at different times postinfection. We used an RNase protection assay to determine the levels of SIN 26S and 49S RNAs because of the relative insensitivity of this method to degradation problems which are often encountered when isolating large RNA molecules from infected cells. Compared with the parental virus, the mutants showed reduced levels of both 26S subgenomic RNA and 49S genomic RNA when the cells were infected at 20 PFU per cell (Fig. 6A). At 2 h postinfection, the 26S and 49S RNA levels of wild-type virus were about twofold higher than those of the sense mutants, fourfold higher than those of the amber mutant, and >10-fold higher than those of the ochre mutant. However, the mutants were nearing wild-type levels of both 26S and 49S RNAs at 5 h postinfection. At an MOI of 20 PFU per cell, the mutants also showed a lag in virus-specific protein synthesis that correlated well with the reduced levels of viral RNAs (Fig. 7). The alterations in RNA and protein synthesis demonstrated by the mutants could be compensated for by infecting the cells at 100 PFU per cell (see Fig. 6B for RNA patterns; data are not shown for protein analyses). These results were reproducible and consistent with the results of the growth rate assay.

Competition assay between wild-type virus and serine mutant. Although at input MOIs of 100 PFU per cell the mutants showed similar growth rates, levels of 26S and 49S RNAs, and protein synthesis patterns, we wished to know whether, even under these conditions, the mutant or the wild-type virus would have a selective growth advantage in mixed infections. The serine mutant was chosen since two bases are changed relative to the wild-type sequence and therefore reversions to the wild type would be less frequent. In addition, the mutant plaques would be more easily distinguished from wild-type plaques by differential hybridization. We developed an in situ plaque hybridization technique to detect specific RNA sequences in the viral genome with 5′-^{32}P-labeled oligonucleotide probes. By using the opal-serine mutagenic oligonucleotide as a probe (20-mer; Fig. 2), the serine mutant plaques could be distinguished from the wild-type plaques in mixed populations. The wild-type virus showed a growth advantage over the serine mutant even at

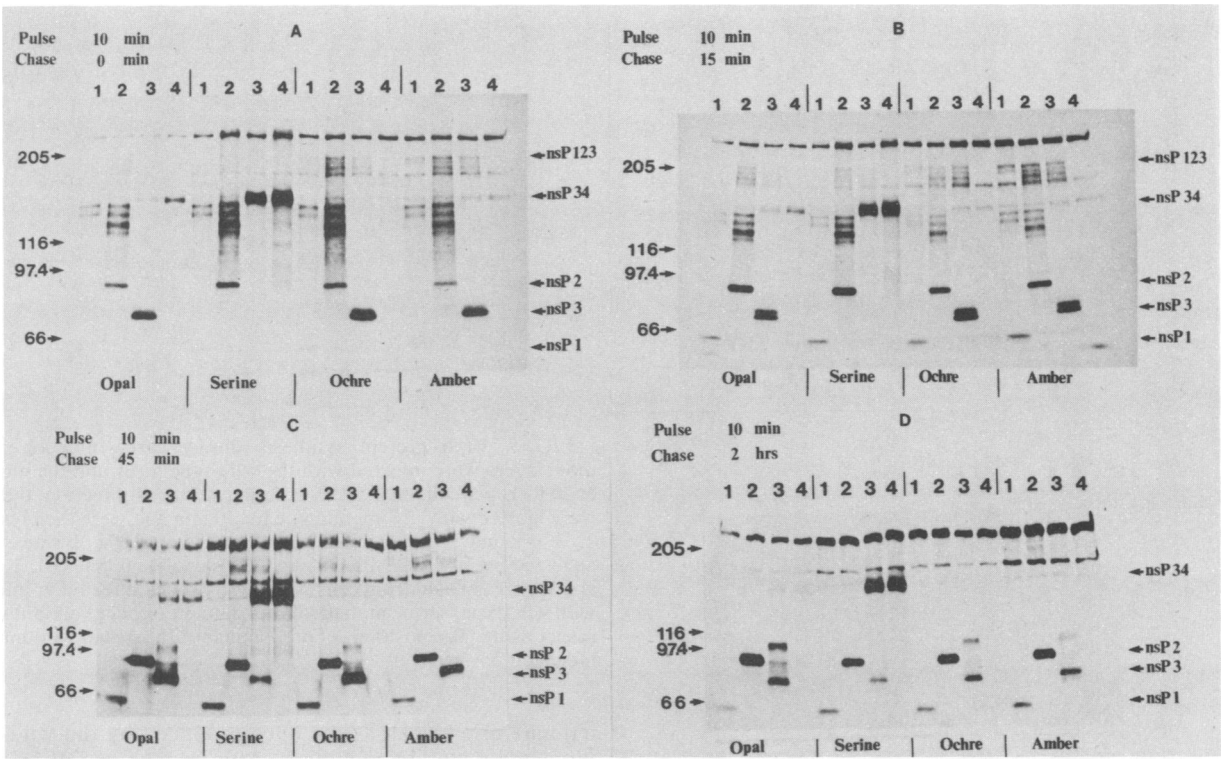

FIG. 5. Immunoprecipitation of viral nonstructural proteins in a pulse-chase experiment. CEF monolayers were infected with wild-type virus (opal) or serine, ochre, or amber mutant virus at 100 PFU per cell. At 4 h postinfection, the cells were pulse-labeled with [^{35}S]methionine for 10 min and chased in the presence of excess unlabeled methionine for 0 (A), 15 (B), 45 (C), or 120 (D) min and were analyzed by 6% SDS-PAGE. The samples in lanes 1, 2, 3, and 4 were immunoprecipitated with SIN antibodies specific to nsP1, nsP2, nsP3, and nsP4, respectively. nsP4 was not detected because of the low levels found in SIN-infected cells (16). Molecular mass standards (in kilodaltons) are indicated on the left, and the positions of the SIN nonstructural proteins are indicated on the right.

100 PFU per cell, and the percentage of serine mutant in the mixed population decreased by about 7 to 8% with each passage (Fig. 8). The serine mutant alone was passaged in parallel as a control, and no significant decrease in positive plaques was found after six passages, suggesting that the mutation was stable upon passaging in CEF. This experiment was also done at a low MOI (0.01 PFU per cell), and again the wild-type virus outcompeted the serine mutant. After six passages, the proportion of serine mutant had decreased from 49 to 4% (data not shown).

Infectivity on different host cell types. To investigate the abilities of different hosts to allow translational readthrough of opal, amber, and ochre codons and to examine other possible host range effects, we tested the abilities of these mutants to grow or form plaques on several different cell types. Cells were infected at 100 PFU per cell (as determined on CEF monolayers), and the media were harvested at either 12 h (for BHK and SW-13) or 24 h (for C7-10) postinfection. All mutants grew on BHK-21 (37°C), SW-13 (37°C), and C7-10 (mosquito cells, 30°C) cells and produced essentially the same yields as that of wild-type virus when titers were determined on CEF cells (data not shown). Although we have not done direct RNA sequencing to confirm that the viruses recovered from amplification in different cell types were the original mutants instead of revertants, some mutants could be distinguished from the wild type by plaque formation and plaque morphologies on these cell types (see below). Furthermore, the wild type and the mutant viruses had no significant difference in plaquing efficiency on each cell type (Table 1), suggesting that it was unlikely that mutant growth was actually due to the presence of revertants in the original stocks.

Both the wild-type virus and each of the five mutants had similar plaque morphologies on BHK-21 cells. The ability to form plaques and the plaque morphologies on the other two cell types, however, were different (Table 2). On mosquito cells (C7-10) at 34.5°C (since SIN shows cytopathic effects in these mosquito cells only at 34.5°C, all of the plaque assays were performed at this temperature), the amber and ochre mutants were unable to form plaques. Under the same conditions, the three sense mutants (serine, tryptophan, and arginine mutants) which overproduced nsP34 could still produce plaques that were indistinguishable from those of the wild-type virus. As mentioned above, the amber and ochre mutants grew well in mosquito cells at 30°C, and the recovered viruses also failed to form plaques on this cell type at 34.5°C, suggesting the retention of the original amber and ochre mutations (data not shown). We then tried to grow amber and ochre mutants at 34.5°C. The resulting virus stocks produced plaques on mosquito cell monolayers with plaquing efficiencies similar to that of the wild-type virus. This result indicated that the amber and ochre mutants grew poorly at this temperature and that variants arose during growth at 34.5°C.

On SW-13 cells, the serine and tryptophan mutants formed plaques larger than those produced by the wild-type virus

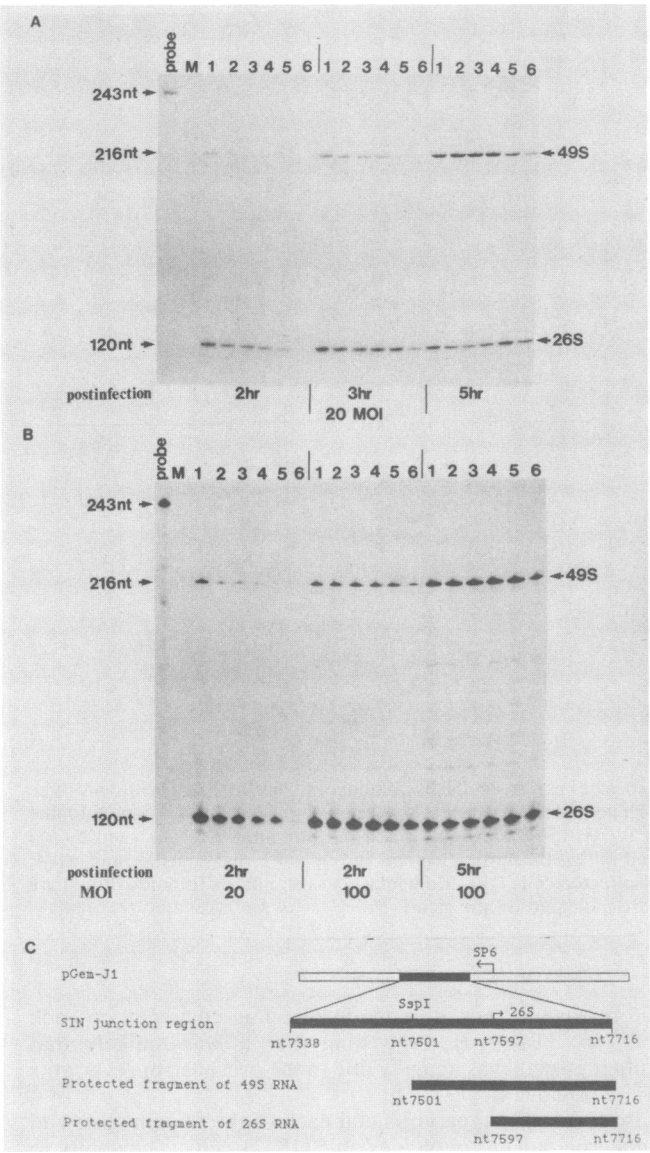

FIG. 6. Viral RNA synthesis during early infection. CEF monolayers were infected with wild-type virus and the five mutants at 20 PFU per cell (A) or 100 PFU per cell (B) (independent experiments). The cytoplasmic RNAs were isolated at 2, 3, and 5 h postinfection, and the levels of 49S and 26S RNAs were determined by an RNase protection assay. The RNA samples in lanes M, 1, 2, 3, 4, 5, and 6 were isolated from cells which were mock infected or infected with wild-type, serine mutant, tryptophan mutant, arginine mutant, amber mutant, or ochre mutant virus, respectively. Major protected RNA fragments for the 49S and 26S RNAs of SIN were 216 and 120 nt, respectively, and are indicated. The minus sense RNA probe (243 nt) was produced by in vitro transcription of *Ssp*I-linearized pGem-J1 as illustrated in panel C. pGem-J1 was constructed by inserting the SIN junction region into the polylinker region of pGem-1 (M. Jones, unpublished data).

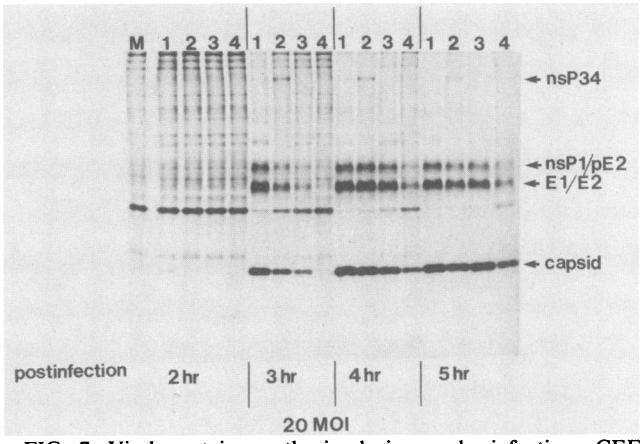

FIG. 7. Viral protein synthesis during early infection. CEF monolayers were infected with the wild-type virus and the mutants at 20 PFU per cell. At 1.5, 2.5, 3.5, and 4.5 h postinfection, the cells were labeled with [^{35}S]methionine for 30 min and were then lysed at 2, 3, 4, and 5 h postinfection, respectively. The lysates were analyzed by 10% SDS-PAGE, and the samples in lanes M, 1, 2, 3, and 4 were isolated from cells which were mock infected or infected with wild-type, serine mutant, amber mutant, or ochre mutant virus, respectively. The positions of predominant SIN-specific proteins are indicated on the right.

and the arginine mutant (plaques formed by the wild-type virus and the arginine mutant were similar in size). The plaque size of the amber mutant was intermediate whereas the ochre mutant stock, on the other hand, produced a heterogeneous population of plaques that were either as large as the ones produced by the serine and tryptophan mutants or as small as the ones produced by the wild-type virus and the arginine mutant. After growth in SW-13 cells, each mutant retained its own plaque morphology (the ochre mutant again produced heterogeneous plaques), indicating that the mutations were fairly stable in this cell type. Protein analysis showed that the nonstructural protein patterns of the mutants were similar to those in CEF cells, i.e., overproduction of nsP34 by the serine, tryptophan, and arginine mutants and underproduction of nsP34 by the amber and ochre mutants (data not shown). Among the heterogeneous plaques of the ochre mutant, the larger plaques were about 10% of the population and were isolated by plaque purification. Sequencing of virus-specific RNAs revealed that the larger plaques were produced by reversions of the ochre codon (UAA) to a glutamine (CAA) or tyrosine (UAU) codon (data not shown). Since the ochre mutant and the wild-type virus had similar plaquing efficiencies on SW-13 cells (for the ochre mutant, both large and small plaques were counted), the data indicate that the original stock of ochre mutant probably already contained a small portion of variants.

DISCUSSION

The in-frame opal termination codon separating the nsP3- and nsP4-coding regions is an interesting feature of the SIN genome and requires that readthrough must occur to translate the nsP4-coding region. On the basis of the mapping of several RNA$^-$ temperature-sensitive mutations to nsP4 (15) and also from the observation that this polypeptide contains amino acid sequences homologous to the RNA-dependent RNA replicase of poliovirus and other putative viral RNA replicases (17, 22, 37), nsP4 sequences appear to be essential for SIN RNA replication. In this report, we investigated the function of the opal codon by studying the phenotypes of SIN mutants in which the opal codon was replaced by either sense amino acid codons (serine, tryptophan, and arginine) or the other two termination codons (amber and ochre). The amino acid at the position corresponding to this opal codon

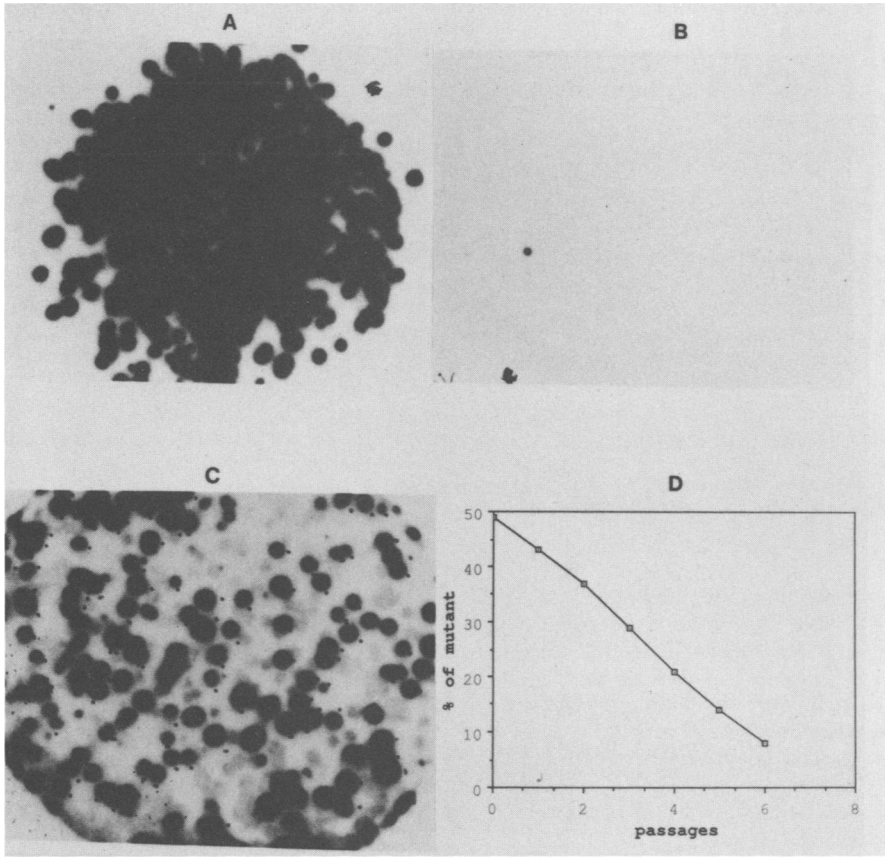

FIG. 8. Competition assay between the wild-type virus and the serine mutant. Mixtures containing equal portions of the wild-type virus and the serine mutant were passaged on CEF monolayers at 100 PFU per cell for six cycles. The titers of the virus stocks obtained from each passage (after 12 h) were determined on CEF monolayers and the plaque lifts were used for in situ hybridization as described in Materials and Methods. The oligonucleotide used for the opal-to-serine mutagenesis was end labeled with ^{32}P and used as a probe. The serine mutant (A) (>500 plaques, positive control), the wild-type virus (B) (>500 plaques, negative control), and viruses from the second passage of mixed infection (C) (499 plaques) are shown. The percentage of serine mutant in the mixed population is illustrated as a function of the passage number (D).

in the cleaved form of nsP3 or the readthrough product nsP34 has not been identified. Of the many possible amino acid replacements, these particular mutations were chosen because (i) serine and tryptophan opal suppressor tRNAs have been isolated from animal cells (see below) and (ii) an arginine residue is found at the location homologous to the opal codon in two other alphaviruses, SFV and O'Nyong-nyong virus (42, 46). Mutants which replaced the opal codon with each of the other two nonsense triplets were made with the thought that these termination codons might modulate the level of the nsP4 domain (either as nsP4 or nsP34) by altering or abolishing readthrough. In vitro transcription of full-length SIN cDNA clones containing these alterations and transfection of CEF monolayers demonstrated that all of these mutant RNAs were infectious with specific infectivities similar to that of the transcripts from the wild-type parental clone.

TABLE 1. Relative plaquing efficiency on different host cells[a]

Cell type	Plaquing efficiency[b]
CEF	100
BHK	20
C7-10[c]	1–1.5
SW-13	0.2–0.3

[a] Wild-type virus and the plaque-forming mutants had similar plaquing efficiencies on each of the cell types shown.
[b] Percent plaquing efficiency relative to that of CEF.
[c] Amber and ochre mutants did not produce plaques on C7-10 monolayers under these conditions.

Analysis of nonstructural protein production by the mutants demonstrated that all of these substitutions led to altered levels of the readthrough product nsP34 compared with that of the wild-type virus. In CEF cells, the mutants with sense replacements greatly overproduced nsP34 while the mutants with either amber or ochre codons underproduced nsP34. The sense replacements also showed a delay in the appearance of nsP3 and reduced levels of this protein. This delay in the production of discrete nsP3 probably reflected the slower production of the C terminus of this protein by cleavage as opposed to translation termination. With the sense opal replacements, we had also expected to find elevated levels of nsP4 if the cleavage separating nsP3 and nsP4 could still occur with reasonable efficiency (as is found with SFV, which lacks the opal codon). Since nsP3 was produced and only a two- to threefold reduction in the

TABLE 2. Plaque formation of wild-type and mutant viruses on C7-10 and SW-13 cells

Virus stock[a]	Plaque formation[b] on:		Plaque phenotype on SW-13[c]
	C7-10	SW-13	
Opal (wild type)	+	+	Small
Serine	+	+	Large
Tryptophan	+	+	Large
Arginine	+	+	Small
Amber	−	+	Intermediate
Ochre	−	+	Small and large[d]

[a] Virus stocks were obtained by transfecting CEF cells with in vitro transcripts, and the mutations were confirmed by direct sequencing of virus-specific RNA.

[b] +, Plaque formation; −, no formation.

[c] The plaque phenotypes of wild-type virus and the plaque-forming mutants on CEF, BHK, and C7-10 cells (amber and ochre mutants did not form plaques on C7-10 cells) were similar.

[d] After 48 h at 37°C, the ochre mutant stock produced both large (2.5-mm diameter) and small plaques (1 mm). The large plaques comprised about 10% of the population.

nsP3 level was found, we conclude that the nsP3-nsP4 cleavage does occur. Elevated synthesis of nsP4, which must have occurred with the sense replacements, appears to have been compensated for by the rapid turnover of nsP4. In wild-type SIN-infected cells, only small amounts of nsP4 can be found by using nsP4-specific antisera and the protein appears to be quite stable (16). These apparently conflicting results can be reconciled if only low levels of nsP4 are required for maximal RNA replication and if excess nsP4, not actively involved in RNA synthesis, is subject to rapid turnover.

Although all five mutants eventually produced yields of virus in CEF cells which were essentially the same as that of the parental virus, it was apparent that RNA synthesis was impaired early in infection at lower MOIs (20 PFU per cell). The amount of both 26S and 49S RNA species was reduced, although the ratio of these species was unchanged. Minus-strand synthesis was not examined, and depressed RNA synthesis could arise from direct effects on plus-strand synthesis or could result from impaired minus-strand synthesis (or both). These defects could stem from the altered levels of nsP3, nsP34, and possibly nsP4 or could result from the amino acid substitutions made for the opal codon by changing the activity of nsP3 or nsP34 or both. For the three sense mutants, the overproduction of nsP34 or the delay of nsP3 synthesis (or reduced amounts) or a combination may have inhibited viral RNA synthesis. The underproduction of nsP34 (possibly of nsP4 also) may contribute to the defects shown by the amber and ochre mutants. These two mutants also showed the most dramatic defects in 49S and 26S RNA synthesis. This observation is consistent with the hypothesis that the RNA-dependent RNA polymerase of SIN resides in nsP4 (22). Since nsP34 rather than nsP4 is the major viral polypeptide that carries the nsP4 protein sequence in SIN-infected cells, it has been suggested that nsP34 is the active form of SIN RNA-dependent RNA polymerase (16, 42). In support of this hypothesis, we have shown that the three sense mutants have different plaque morphologies on SW-13 cells, even though the nonstructural protein patterns were similar to those in CEF (data not shown). Since the only difference in these three mutants is that the opal codon is replaced by different amino acid codons, this suggests that nsP34 could be a functional protein and that the nsP34 of the arginine mutant somehow leads to the small-plaque phenotype observed in SW-13 cells. We cannot rule out, however, the possibility that these differences were due to the effects of the amino acid substitutions on the function of nsP3 itself. For tobacco mosaic virus, it has been reported that the readthrough product (putative viral RNA replicase) may function in the form of a 183-kilodalton polyprotein (13, 17, 22, 34) and no cleaved readthrough product has ever been observed. In addition, Ishikawa et al. (20) demonstrated that sense replacement of the in-frame amber codon of tobacco mosaic virus with tyrosine still produces infectious virus, supporting the hypothesis that the 183-kilodalton polyprotein of tobacco mosaic virus is functional by itself. It is possible that nsP34 of SIN could also function as the viral RNA replicase without being cleaved into nsP4. However, it is clear that small amounts of nsP4 can be found in SIN-infected cells (16), and both nsP34 and nsP4 may have functional roles in SIN RNA replication.

Although no definitive conclusions can be drawn from these studies concerning the molecular mechanisms by which altered levels of these nonstructural proteins lower the efficiency of RNA synthesis, several observations are worth noting. Since the specific infectivities of the mutant transcripts were essentially similar to that of the wild-type transcripts, these mutations have not dramatically affected the ability of the incoming genome to switch from being translated to initiating RNA replication. It is of interest that the defects shown by the mutants at 20 PFU per cell can be overcome by infecting the cells at higher MOIs (100 PFU per cell). For the wild-type parent, increasing the MOI above 20 PFU per cell does not result in detectable increases in the levels of virus-specific RNAs even at 2 h postinfection. This finding indicates that the opal replacement mutations lead to limiting amounts of one or more essential replicase components and that increasing the number of incoming genome RNAs per cell can partially compensate for this defect. For the serine mutant, the defect relative to the wild-type virus was also evident in growth competition experiments. Even at high-input MOIs (100 PFU per cell), the serine mutant defect was not compensated for by wild-type replicase components. If a limited number of sites are available in the host cell for the assembly of replication complexes, this indicates that the serine mutant may not assemble these complexes as efficiently as does the wild-type virus. Consistent with the low complementation efficiencies typically observed with SIN mutants temperature-sensitive for RNA synthesis (6), these results also indicate that the nonstructural proteins of SIN do not function efficiently in *trans*. It seems plausible that the nonstructural proteins translated from an incoming viral genomic RNA might be preferentially used for the assembly of that RNA into a replication complex. It is unknown whether this *cis* effect simply reflects diffusion-limited assembly of the replicase components or a more ordered mechanism in which translated nonstructural proteins rapidly associate with their mRNA and eventually initiate replication of that RNA.

The opal substitution mutants also exhibited different plaque morphologies and growth properties in different host cell types including chicken, hamster, human, and mosquito cells. The most dramatic effect was seen in mosquito cells (C7-10), in which the amber and ochre mutants were temperature sensitive and grew well at 30°C but not at 34.5°C. This host-dependent temperature-sensitive phenotype may be a direct effect of lower levels of the nsP4 domain (although this has not been examined directly in C7-10 cells). Alternatively, different amounts of the nsP4 domain may be present at the two temperatures, resulting from temperature-

dependent effects on readthrough efficiencies of the amber and ochre codons. In future experiments, it will be of interest to examine the nonstructural protein patterns and the RNA phenotypes of these mutants in mosquito cells at the permissive and restrictive temperatures. In human cells (SW-13), the overproduction of nsP34 may contribute to the large-plaque morphology seen for the serine and tryptophan mutants (larger than that of the wild type). Interestingly, the arginine mutant, which also overproduces nsP34 in this cell type (data not shown), produced smaller plaques. As discussed above, this observation could be interpreted as evidence for nsP34 as a functional component of the RNA replication machinery.

The question still arises as to why some alphaviruses possess the opal codon separating nsP3 and nsP4 (SIN, Ross River virus, and Middelburg virus) and others do not (SFV and O'Nyong-nyong virus). Within the limited set of SIN mutants examined here, the wild-type virus containing the opal codon was more efficient at virus replication than any of the mutants in CEF, but this advantage was rather subtle and most apparent at a low MOI. As shown in the growth competition experiments, after multiple passages at either a high or a low MOI, such an advantage is easily selected and the wild-type virus quickly predominates the population. Thus, for SIN the opal codon appears to be advantageous, with the likely function being regulation of the level of nsP34 rather than nsP4. For the other alphaviruses, in which arginine is found in place of the opal codon, the level of nsP34 may be regulated by alternative mechanisms such as nsP34 cleavage efficiency. In SFV-infected cells, higher levels of nsP4 are found (24; unpublished data). If this observation is of functional significance, it suggests that different levels of nsP4 may be required by different alphaviruses for optimal RNA replication. It will be interesting to examine the effect of a parallel set of mutations for SFV or O'Nyong-nyong virus when an infectious cDNA clone becomes available.

Although the mechanism for the opal suppression of SIN remains unknown, there are two classical mechanisms by which readthrough of terminations codons can occur: (i) suppression by specific suppressor tRNAs and (ii) readthrough by normal cytoplasmic tRNAs through misreading. Naturally occurring opal suppressor tRNAs have been discovered in a variety of animal cells (9, 12, 19) that insert either serine or tryptophan in response to the opal codon. However, it has been suggested that misreading is the major mechanism for natural suppression in higher eucaryotes, while suppressor tRNAs may be involved in some specialized cellular functions (18). In this study, we have demonstrated that both amber (UAG) and ochre (UAA) codons can be leaky in CEF cells (as confirmed by directly sequencing replicated viral RNAs). This also seems to be the case for BHK-21 cells (hamster), C7-10 cells (mosquito), and SW-13 cells (human), considering the ability of amber and ochre mutants to replicate in these cells (this assumes, as discussed above, that the nsP4-coding region is required for SIN replication). This appears to be the first evidence of ochre codon readthrough in animal cells. In future studies, it will be of interest to determine which amino acid(s) is inserted in response to these termination codons.

In addition to those of alphaviruses, other viral mRNAs as well as some cellular messages use readthrough of termination codons to synthesize essential translation products. This suggests another important level in the regulation of gene expression via translational readthrough of termination codons. In addition to tobacco mosaic virus, some retroviruses (e.g., Moloney murine leukemia virus) use translation of an in-frame UAG codon to produce viral reverse transcriptase (13, 34, 35, 53, 54). Recently, an in-frame opal codon has been found to encode a selenocysteine residue essential for certain enzymatic activities found in both procaryotic and eucaryotic organisms (7, 57). Readthrough of termination codons can be facilitated by many factors, including the nucleotide sequences around the termination codons, so-called "codon context" (11). In the SIN genome, the opal codon is followed by a cytosine residue. According to a compilation study (25), this nucleotide does not typically follow termination codons in eucaryotic organisms. It will be of interest to determine whether readthrough of the SIN opal codon separating nsP3 and nsP4 is facilitated by this context or other nucleotide contexts.

ACKNOWLEDGMENTS

We thank Robert E. Johnston and Victor Stollar for providing BHK-21 and C7-10 cells, respectively; W. Reef Hardy and James H. Strauss for SIN antibodies specific to nsP1-4; Douglas Berg for plasmid pGC2 and phage M13k07; M. Jones for plasmid pGEM-J1; and Henry V. Huang, Milton J. Schlesinger, Sondra Schlesinger, James H. Strauss, and members of the laboratory for helpful suggestions on the manuscript.

This work was supported by Public Health Service grant AI24134 from the National Institutes of Health and by a grant from the Pew Memorial Trust. G.L. is supported by a predoctoral fellowship from the Josiah Macy Foundation to the Division of Biology & Biomedical Sciences of Washington University. C.M.R. is a Pew Scholar in the Biomedical Sciences.

LITERATURE CITED

1. **Anderson, D. J., and G. Blobel.** 1983. Immunoprecipitation of proteins from cell-free translations. Methods Enzymol. **96:** 111–120.
2. **Barton, D. J., S. G. Sawicki, and D. L. Sawicki.** 1988. Demonstration in vitro of temperature-sensitive elongation of RNA in Sindbis virus mutant *ts*6. J. Virol. **62:**3597–3602.
3. **Bresser, J., J. Doering, and D. Gillespie.** 1983. Selective mRNA or DNA immobilization from whole cells. DNA **2:**243–254.
4. **Brun, G., and N. Plus.** 1980. The viruses of *Drosophila*, p. 625–702. *In* M. Ashburner and T. R. F. Wright (ed.), The genetics and biology of *Drosophila*, vol. 2. Academic Press, Inc., New York.
5. **Burge, B. W., and E. R. Pfefferkorn.** 1966. Isolation and characterization of conditional-lethal mutants of Sindbis virus. Virology **30:**204–213.
6. **Burge, B. W., and E. R. Pfefferkorn.** 1966. Complementation between temperature-sensitive mutants of Sindbis virus. Virology **30:**214–223.
7. **Chambers, I., J. Frampton, P. Goldfarb, N. Affara, W. McBain, and P. R. Harrison.** 1986. The structure of the mouse glutathione peroxidase gene: the selenocysteine in the active site is encoded by the 'termination' codon, TGA. EMBO J. **5:**1221–1227.
8. **Clark, H. F., M. M. Cohen, and P. D. Lunger.** 1973. Comparative characterization of a C-type virus-producing cell line (VSW) and a virus-free cell line (VH2) from *Vipera russelli*. J. Natl. Cancer Inst. **51:**645–654.
9. **Diamond, A., B. Dudock, and D. Hatfield.** 1981. Structure and properties of a bovine liver UGA suppressor serine tRNA with a tryptophan anticodon. Cell **25:**497–506.
10. **Durbin, R. K., and V. Stollar.** 1984. A mutant of Sindbis virus with a host-dependent defect in maturation associated with hyperglycosylation of E2. Virology **135:**331–344.
11. **Engelberg-Kulka, H.** 1981. UGA suppression by normal $tRNA^{Trp}$ in *Escherichia coli*: codon context effects. Nucleic Acids Res. **9:**983–991.
12. **Geller, A. I., and A. Rich.** 1980. A UGA termination suppression $tRNA^{Trp}$ active in rabbit reticulocytes. Nature (London)

283:41–46.
13. **Goelet, P., G. P. Lomonossoff, P. J. G. Butler, M. E. Akam, M. J. Gait, and J. Karn.** 1982. Nucleotide sequence of tobacco mosaic virus RNA. Proc. Natl. Acad. Sci. USA **79**:5818–5822.
14. **Guilley, H., J. C. Carrington, E. Balazs, G. Jonard, K. Richards, and T. J. Morris.** 1985. Nucleotide sequence and genome organization of carnation mottle virus RNA. Nucleic Acids Res. **13**:6663–6677.
15. **Hahn, Y. S., A. Grakoui, C. M. Rice, E. G. Strauss, and J. H. Strauss.** 1989. Mapping of RNA-temperature-sensitive mutants of Sindbis virus: complementation group F mutants have lesions in nsP4. J. Virol. **63**:1194–1202.
16. **Hardy, W. R., and J. H. Strauss.** 1988. Processing the nonstructural polyproteins of Sindbis virus: study of the kinetics in vivo by using monospecific antibodies. J. Virol. **62**:998–1007.
17. **Haseloff, J., P. Goelet, D. Zimmern, P. Ahlquist, R. Dasgupta, and P. Kaesberg.** 1984. Striking similarities in amino acid sequence among nonstructural proteins encoded by RNA viruses that have dissimilar genomic organization. Proc. Natl. Acad. Sci. USA **81**:4358–4362.
18. **Hatfield, D.** 1985. Suppression of termination codons in higher eukaryotes. Trends Biochem. Sci. **10**:201–204.
19. **Hatfield, D. L., B. S. Dudock, and F. C. Eden.** 1983. Characterization and nucleotide sequence of a chicken gene encoding an opal suppressor tRNA and its flanking DNA segments. Proc. Natl. Acad. Sci. USA **80**:4940–4944.
20. **Ishikawa, M., T. Meshi, F. Motoyoshi, N. Takamatsu, and Y. Okada.** 1986. *In vitro* mutagenesis of the putative replicase genes of tobacco mosaic virus. Nucleic Acids Res. **14**:8291–8305.
21. **Johnston, R. E., and J. F. Smith.** 1988. Selection for accelerated penetration in cell culture coselects for attenuated mutants of Venezuelan equine encephalitis virus. Virology **162**:437–443.
22. **Kamer, G., and P. Argos.** 1984. Primary structural comparison of RNA-dependent polymerases from plant, animal and bacterial viruses. Nucleic Acids Res. **12**:7269–7282.
23. **Keränen, S., and L. Kääriäinen.** 1979. Functional defects of RNA-negative temperature-sensitive mutants of Sindbis and Semliki Forest viruses. J. Virol. **32**:19–29.
24. **Keränen, S., and L. Ruohonen.** 1983. Nonstructural proteins of Semliki Forest virus: synthesis, processing, and stability in infected cells. J. Virol. **47**:505–551.
25. **Kohli, J., and H. Grosjean.** 1981. Usage of the three termination codons: compilation and analysis of the known eukaryotic and prokaryotic translation termination sequences. Mol. Gen. Genet. **182**:430–439.
26. **Laemmli, U. K.** 1970. Cleavage of structural proteins during the assembly of the head of bacteriophage T4. Nature (London) **227**:680–685.
27. **Laskey, R. A., and A. D. Mills.** 1975. Quantitative film detection of ^{3}H and ^{14}C in polyacrylamide gels by fluorography. Eur. J. Biochem. **56**:335–341.
28. **Leake, C. J., M. G. R. Varma, and M. Pudney.** 1977. Cytopathic effect and plaque formation by arboviruses in a continuous cell line (XTC-2) from the toad *Xenopus laevis*. J. Gen. Virol. **35**:335–339.
29. **Maniatis, T., E. F. Fritsch, and J. Sambrook.** 1982. Molecular cloning: a laboratory manual. Cold Spring Harbor Laboratory, Cold Spring Harbor, N.Y.
30. **Maxam, A. M., and W. Gilbert.** 1980. Sequencing end-labeled DNA with base-specific chemical cleavages. Methods Enzymol. **65**:499–560.
31. **Melton, D. A., P. A. Krieg, M. R. Rebagliati, T. Maniatis, K. Zinn, and M. R. Green.** 1984. Efficient *in vitro* synthesis of biologically active RNA and RNA hybridization probes from plasmids containing a bacteriophage SP6 promoter. Nucleic Acids Res. **12**:7035–7056.
32. **Myers, R. M., L. S. Lerman, and T. Maniatis.** 1985. A general method for saturation mutagenesis of cloned DNA fragments. Science **229**:242–247.
33. **Nakamaye, K. L., and F. Eckstein.** 1986. Inhibition of restriction endonuclease Nci I cleavage by phosphorothioate groups and its application to oligonucleotide-directed mutagenesis. Nucleic Acids Res. **14**:9679–9698.
34. **Pelham, H. R. B.** 1978. Leaky UAG termination codon in tobacco mosaic virus RNA. Nature (London) **272**:469–471.
35. **Philipson, L., P. Anderson, U. Olshevsky, R. Weinberg, and D. Baltimore.** 1978. Translation of MuLV and MSV RNAs in nuclease-treated reticulocyte extracts: enhancement of the gag-pol polypeptide with yeast suppressor tRNA. Cell **13**:189–199.
36. **Rice, C. M., R. Levis, J. H. Strauss, and H. V. Huang.** 1987. Production of infectious RNA transcripts from Sindbis virus cDNA clones: mapping of lethal mutations, rescue of a temperature-sensitive marker, and in vitro mutagenesis to generate defined mutants. J. Virol. **61**:3809–3819.
37. **Rice, C. M., E. G. Strauss, and J. H. Strauss.** 1986. Structure of the flavivirus genome, p. 279–326. *In* S. Schlesinger and M. J. Schlesinger (ed.), The Togaviridae and Flaviviridae. Plenum Publishing Corp., New York.
38. **Sanger, F., S. Nicklen, and A. R. Coulson.** 1977. DNA sequencing with chain-terminating inhibitors. Proc. Natl. Acad. Sci. USA **74**:5463–5467.
39. **Sawicki, D. L., S. G. Sawicki, S. Keränen, and L. Kääriäinen.** 1981. Specific Sindbis virus-coded function for minus-strand RNA synthesis. J. Virol. **39**:348–358.
40. **Shinnick, T. M., R. A. Lerner, and J. G. Sutcliffe.** 1981. Nucleotide sequence of Moloney murine leukemia virus. Nature (London) **293**:543–548.
41. **Strauss, E. G., E. M. Lenches, and J. H. Strauss.** 1976. Mutants of Sindbis virus. I. Isolation and partial characterization of 89 new temperature-sensitive mutants. Virology **74**:154–168.
42. **Strauss, E. G., R. Levinson, C. M. Rice, J. Dalrymple, and J. H. Strauss.** 1988. Nonstructural proteins nsP3 and nsP4 of Ross River and O'Nyong-nyong viruses: sequence and comparison with those of other alphaviruses. Virology. **164**:265–274.
43. **Strauss, E. G., C. M. Rice, and J. H. Strauss.** 1983. Sequence coding for the alphavirus nonstructural proteins is interrupted by an opal termination codon. Proc. Natl. Acad. Sci. USA **80**:5271–5275.
44. **Strauss, E. G., C. M. Rice, and J. H. Strauss.** 1984. Complete nucleotide sequence of the genomic RNA of Sindbis virus. Virology **133**:92–110.
45. **Strauss, E. G., and J. H. Strauss.** 1986. Structure and replication of the alphavirus genome, p. 35–90. *In* S. Schlesinger and M. J. Schlesinger (ed.), The Togaviridae and Flaviviridae. Plenum Publishing Corp., New York.
46. **Takkinen, K.** 1986. Complete nucleotide sequence of the nonstructural protein genes of Semliki Forest virus. Nucleic Acids Res. **14**:5667–5682.
47. **Taylor, R. M., H. S. Hurlbut, T. H. Work, J. R. Kingston, and T. E. Frothingham.** 1955. Sindbis virus: a newly recognized arthropod-transmitted virus. Am. J. Trop. Med. Hyg. **4**:844–862.
48. **Vieira, J., and J. Messing.** 1987. Production of single-stranded plasmid DNA. Methods Enzymol. **153**:3–11.
49. **Villarreal, L. P., and P. Berg.** 1977. Hybridization in situ of SV40 plaques: detection of recombinant SV40 virus carrying specific sequences of nonviral DNA. Science **196**:183–186.
50. **Weiner, A. M., and K. Weber.** 1971. Natural readthrough at the UGA termination signal of Qβ coat protein cistron. Nature (London) New Biol. **234**:206–209.
51. **Weislander, L.** 1979. A simple method to recover intact high molecular weight RNA and DNA after electrophoretic separation in low gelling temperature agarose gels. Anal. Biochem. **98**:305–309.
52. **Weiss, B., R. Rosenthal, and S. Schlesinger.** 1980. Establishment and maintenance of persistent infection by Sindbis virus in BHK cells. J. Virol. **33**:463–474.
53. **Yoshinaka, Y., I. Katoh, T. D. Copeland, and S. Oroszlan.** 1985. Murine leukemia virus protease is encoded by the gag-pol gene and is synthesized through suppression of an amber termination codon. Proc. Natl. Acad. Sci. USA **82**:1618–1622.
54. **Yoshinaka, Y., I. Katoh, T. D. Copeland, and S. Oroszlan.** 1985. Translational readthrough of an amber termination codon during synthesis of feline leukemia virus protease. J. Virol. **55**:870–873.
55. **Zimmern, D., and P. Kaesberg.** 1978. 3′-Terminal nucleotide

sequence of encephalomyocarditis virus RNA determined by reverse transcriptase and chain-terminating inhibitors. Proc. Natl. Acad. Sci. USA **75**:4257–4261.

56. **Zinn, K., D. DiMaio, and T. Maniatis.** 1983. Identification of two distinct regulatory regions adjacent to the human β-interferon gene. Cell **34**:865–879.
57. **Zinoni, F., A. Birkmann, W. Leinfelder, and A. Böck.** 1987. Cotranslational insertion of selenocysteine into formate dehydrogenase from *Escherichia coli* directed by a UGA codon. Proc. Natl. Acad. Sci. USA **84**:3156–3160.
58. **Zoller, M. J., and M. Smith.** 1982. Oligonucleotide-directed mutagenesis using M13-derived vectors: an efficient and general procedure for the production of point mutations in any fragment of DNA. Nucleic Acids Res. **10**:6487–6500.